Journal of Mines, Metals and Fuels, *71(11): 2278-2288; 2023. DOI: 10.18311/jmmf/2023/36048*

Print ISSN : 0022-2755

Journal of Mines, Metals and Fuels

**Contents available at:** *www.informaticsjournals.com/index.php/jmmf*

# A Study on Heat and Flow of Viscoelastic Dielectric Liquid Over an Inclined Stretching Sheet

**N. Veena[1,4]*, Annamma Abraham[2,4], Jojy Joseph Idicula[2,4] and P. A. Dinesh[3,4]**

[1]*Department of Mathematics, SJC Institute of Technology, Chickballapur – 562101, Karnataka, India; veena80research@gmail.com*

[2]*Department of Mathematics, BMS Institute of Technology and Management, Bengaluru – 560064, Karnataka, India*

[3]*Department of Mathematics, M.S. Ramaiah Institute of Technology, Bengaluru – 560054, Karnataka, India*

[4]*Department of Mathematics, Visvesveraya Technological University, Belagavi – 590018, Karnataka, India*

## Abstract

*Exploring the behavior of viscoelastic dielectric liquids on an inclined stretching sheet involves a comprehensive mathematical analysis. Employing a Runge-Kutta-based shooting strategy, this study delves into the system's non-linear Ordinary Differential Equations (ODEs). The research investigates how physical parameters like the Prandtl number, dielectric interaction parameter, viscoelastic parameter, Grashof number, and angle of inclination influence both velocity and temperature. Through graphical representations, the study sheds light on the impact of these factors and compares its findings with existing data. This intriguing combination of dielectric liquid behaviour under varying inclinations holds significant potential applications in Mines, Materials, and Fuels.*

**Keywords:** *Angle of Inclination, Dielectric liquid, Stretching Sheet.*

## 1.0 Introduction

Non-Newtonian fluids play a pivotal role across diverse industries like nuclear reactors, metallurgy, textile manufacturing, geothermal engineering, space technology, and crystal growth. Their boundary layer flow holds immense significance due to their widespread use in various sectors. From nuclear reactors and metallurgical processes to fiber spinning, metal casting, space technology, and crystal development, non-Newtonian fluids find multifaceted applications. The exploration of dielectric liquid flow over an inclined stretching viscoelastic sheet opens doors to valuable applications in science, technology, industrial equipment, electrical devices, and the automotive sector, among others. Non-Newtonian fluids models are used, among other things, in the fabrication of plastics, polymers, optical fibers, hot rolling, drilling mud, cooling metallic plates, paper manufacturing, metal spinning, etc. which comes under the field of materials. Not only this, stretching sheet applications can be found in the field of mining. In mineral processing, stretching a sheet of fluid flow can be used in techniques like froth flotation, where the stretching of the fluid sheet helps separate minerals from ore on their hydrophobicity. Stretching fluid flow aid in hydraulic mining processes where high-pressure water jets are used to dislodge and transport materials, facilitating the separation of minerals from the surrounding rock.

Various scientific disciplines have extensively explored the boundary layer flow of actual liquids passing over stretched sheets, evident in polymer sheet extrusion, metallurgy, and chemical engineering. Manufacturers of these materials aim to stretch them from a slit to a specific shape, wherein the cooling rate significantly

*Author for correspondence

impacts the desired qualities of the final product. To manage this cooling rate and optimize the desired characteristics, electrically conductive fluids come into play. The author emphasized the pivotal role of stretching in plastic extrusion, highlighting its critical importance in the process[1]. There's been extensive exploration into understanding the dynamics of boundary layers along continuous solid surfaces and flat planes[2,3]. Through experiments, scholars have unveiled the characteristics of laminar and turbulent boundary layers along a continuously moving cylindrical surface. This discovery sheds light on the behavior of these boundary layers in such dynamic settings[4]. Both analytical techniques and experimental approaches have been employed to investigate the flow and temperature fields within the boundary layer of a continuously moving surface. This comprehensive examination offers insights into the dynamics of this particular flow regime[5]. The discussion involves a mathematical formulation describing the steady boundary layer flow generated by the linear stretching of an elastic sheet in its plane. This stretching occurs at a velocity that increases linearly as the distance from a fixed point grows[6]. The equation of motion governing the boundary layer flow over a stretched plate was tackled using the Crane's model and the Walters' liquid B model, which represents a viscoelastic fluid[7]. Additionally, there was a separate investigation into the behavior of incompressible second-order fluid flow across a stretching sheet that was documented[8].

This research holds significance for multiple polymer processing methods, particularly in the continuous extrusion of polymer sheets from a die. Notably, when keeping the wall and ambient temperatures constant, an intriguing observation emerged: as the thermal conductivity (k) increases, there's a noticeable rise in temperature at specific locations, while the Prandtl number remains relatively stable or consistent[9].

In investigating the flow of a viscous ferrofluid over a stretching sheet, the inclusion of a magnetic dipole factor is notable. By formulating momentum and thermal energy equations as a five-parameter problem, the study reveals that the magnetic field has a substantial impact: it alters flow velocity and notably diminishes the rate of heat transfer on the stretching sheet[10]. Analyzing the way heat moves across an extended surface involves looking at two different situations: one where the surface has a set temperature and another where it has a specific heat flow at the wall. To do this, researchers use Kummer's functions, especially suited for surfaces that resemble parabolic cylinders with a boundary layer that generally stays quite broad. Moreover, the research also shows that for low Prandtl values, there isn't a solution resembling a boundary layer[11].

There's an exploration into the behavior of incompressible, electrically conducting viscoelastic fluids as they traverse an elastic porous sheet[12]. In the context where an Oldroyd-B fluid occupies the area above an elastic sheet undergoing stretching, alongside a constant free-stream velocity, a method employing a similarity transformation is applied. This transformation applies to both the velocity field and the three components of the stress tensor. By employing this technique, the governing equations are simplified, resulting in a system of coupled nonlinear ordinary differential equations. These equations are then approached through numerical solutions, utilizing Weissenberg number perturbation as a methodology[13].

A study investigates the stability of a viscoelastic dielectric liquid when subjected to a vertical electric field in the presence of a temperature gradient[14]. The article delves into the thermal instability arising within a layer of dielectric liquid when subjected to synchronous or asynchronous temperature variations along its boundary[15]. The author investigated the boundaries of a dielectric fluid layer under the influence of small-amplitude, time-periodic body forces[16]. employing a systematic approach to examine subtle nonlinear effects, the study delved into the influence of time-based oscillations within the Rayleigh-Bénard system on heat transfer behaviors in dielectric liquids[17]. Exploring the Rayleigh-Bénard-Marangoni instability in micro-polar dielectric fluids, the researcher employed the Galerkin technique[18]. Another investigation focused on the flow of ferrofluids, specifically over an inclined stretched surface affected by a magnetic dipole. Here, the ferromagnetic interaction parameter emerged as a critical factor for effectively achieving the desired temperature outcomes.[19].

A study explores the effects of thermal radiation, velocity slip, and mass convective boundary conditions on non-Newtonian heat transfer analysis. Within this research, an intriguing finding is unveiled: as the parameters for velocity slip and fluid material increase, the

velocity field diminishes accordingly[20]. The significance of Jeffery fluid lies in its ability to influence the flow velocity of material, a characteristic not exhibited by the Oldroyd-B fluid. Interestingly, despite this, the Jeffery fluid showcases lower velocities at higher porosity values compared to the Oldroyd-B fluid. Furthermore, in terms of material transfer in a liquid phase, the Jeffery liquid outperforms the Oldroyd-B liquid, displaying slower decay rates[21].

A study on Maxwell's hybrid nanoliquid found that magnetic fields can be successfully used for controlling the flow behaviour of a liquid[22]. Upon observation of the boundary layer, a notable deduction emerges: the velocity profile experiences a decrease when influenced by both a magnetic field and a slip condition. This finding holds significant implications across diverse applications such as polymer fluid extrusion, liquid crystal solidification, wood coating, biocompatibility, bio-imaging, and biosensors, among others[23]. A recent study delved into the combined impacts of chemical reactions, thermal radiation, and electromagnetic forces on the flow of hydromagnetic water over an exponentially stretching sheet. This investigation explores an innovative cooling method employed in nuclear fission reactors. Instead of using conventional cooling tubes, it involves circulating liquid sodium throughout the reactor's main body. This cooling technique has diverse applications, ranging from cooling infinite hot metal sheets in cooling tubs to the production of rubber sheets, fabrics, wire cables, and fiberglass sheets. Additionally, microwaves are utilized to facilitate the circulation of liquid sodium, essential for effective cooling within nuclear reactors and various manufacturing processes[24]. The discussion highlighted the diverse applications of stretching sheets across various fields such as science, metallurgy, and polymer sheet extrusion. The findings revealed intriguing relationships between key parameters and flow characteristics: increasing the magnetic parameter led to a decline in velocity profiles. Moreover, elevating the Prandtl and Schmidt values resulted in reduced temperature and concentration profiles within the flow zone. Notably, an increase in the Maxwell fluid parameter caused a shift in velocity profiles and amplified the temperature field. Additionally, in laminar flow conditions, raising the Soret number accentuated the visibility of concentration profiles[25].

Non-Newtonian fluids find versatile applications across industries, serving purposes ranging from safeguarding feet in footwear to playing crucial roles in food and pharmaceutical manufacturing. Additionally, these fluids are integral in processes like cooling liquid metal during casting, showcasing their wide-ranging utility in various industrial operations. The primary findings of the investigation are that temperature increases with radiation and thermophoretic parameters, velocity slows down with an increase in Maxwell and magnetic parameters, and motile microorganisms are a declining function of Peclect and bio-convection Lewis numbers[26]. Research investigates the flow of fluids doped with ferromagnetic elements over an elastic sheet. The study's proposal suggests that the inclusion of Brownian motion enhances the thermal gradient, particularly in the presence of Stefan's blowing condition[27].

The research concludes that leveraging magnetic dipoles and thermophoretic particle deposition could enhance the flow characteristics of Maxwell liquid over a stretched sheet. The improvements in the ferromagnetic interaction parameter suggest a reduction in the velocity gradient alongside heightened rates of mass and heat transfer[28]. A study gives evidence that when the ferromagnetic interaction parameter and Maxwell parameter are different, radial velocity will decline. Large temperature profile surges are seen for the increase of the Biot number and radiation parameters for the hybrid nano-liquid[29]. The study revealed that when magnets and suction are introduced, the fluid's movement decelerates, accompanied by an elevation in viscosity, resulting in a perceptible sensation of increased "stickiness"[30]. A study highlights that heating nanofluids enhances their efficiency notably. The Nusselt number, a crucial measure in heat transfer, displays increments attributed to both Brownian motion and unsteadiness. Interestingly, in contrast to Maxwell fluids, Newtonian liquids demonstrate enhanced thermal performance with increases in volume percentage and the ferromagnetic interaction parameter. Additionally, significant volume fractions and thermal relaxation parameters coincide with heightened rates of heat transmission and an amplified skin friction coefficient[31]. The effect of variation of various parameter on flow and heat transfer is discussed and concluded that as the Prantl number grows heat transfer decreases whereas opposite behavior can be observed as viscoelastic

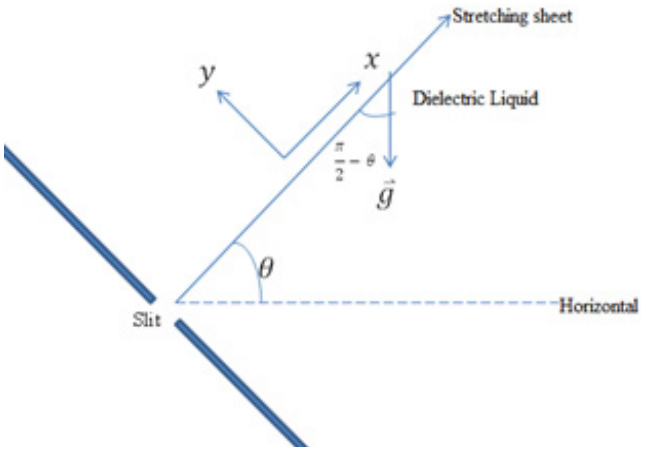


**Figure 1.** Mathematical modelling of the fluid flow.

parameter increases and dielectric liquid can be used efficiently to decrease the heat transform[32].

In the existing literature, numerous authors have explored the dynamics of ferrofluid flow and heat transfer under magnetic fields. This research, however, focuses on investigating the flow and heat transfer of a viscoelastic dielectric liquid along an inclined stretched sheet under the influence of an electric field. The study involves a numerical analysis of the flow induced by a stretched sheet in a dielectric liquid. To tackle the governing nonlinear partial differential equations, dimensionless variables are employed, transforming them into nonlinear ordinary differential equations. These equations are solved numerically using a shooting iteration approach and the fourth-order Runge-Kutta integration scheme.

Imagine a scenario where a smooth, unyielding surface is tilted at an angle θ to the horizontal, causing a continuous flow of an incompressible, non-conducting liquid. This flow, devoid of any heat transfer, is directed by balanced forces along the x and y axes, effectively counteracting gravity's influence. The surface undergoes controlled stretching, its velocity $u_w(x) = cx$ gradually increasing with distance from the starting point. Adding to this setup, an electric dipole is positioned at a distance from the x-axis, placed some distance away from the surface along the y-axis. These parameters define the governing principles governing this specific physical arrangement.

$$\frac{\partial u}{\partial x}+\frac{\partial v}{\partial y}=0 \tag{1}$$

$$u\frac{\partial u}{\partial x}+v\frac{\partial u}{\partial y}+\lambda_1\left[u^2\frac{\partial^2 u}{\partial x^2}+v^2\frac{\partial^2 u}{\partial y^2}+2uv\frac{\partial^2 u}{\partial x\,\partial y}\right]=\frac{P}{\rho}\frac{\partial E}{\partial x}+\mathcal{V}\frac{\partial^2 u}{\partial y^2}+g\beta^*(T_c-T)sin\theta \tag{2}$$

$$u\frac{\partial T}{\partial x}+v\frac{\partial T}{\partial y}-\frac{K}{\rho C_P}\frac{\partial^2 T}{\partial y^2}=\frac{K}{\rho C_P}\left[\mu\left(\frac{\partial u}{\partial x}\right)^2+2\mu\left(\frac{\partial v}{\partial y}\right)^2\right] \tag{3}$$

The symbols and terms used are explained in the nomenclature section for reference.

The boundary conditions are considered to be at a Prescribed Surface Temperature (PST) is

$u(x,0)=cx, v(x,0)=0$ and

$$T(x,0)=T_w=T_c-A\left(\frac{x}{L}\right)\ in\ PST \tag{4}$$

The positive constant 'A' holds significance, while $L=\sqrt{\frac{v}{c}}$ represents the characteristic length.

The various significant denotations on temperature are

'T' denotes the temperature of the fluid

'$T_w$' stands for the temperature of the stretching sheet

'$T_c$' represents the Curie temperature

The dielectric liquid's flow is affected by the electric field created by the nearby electric dipole. A particular source gives rise to the scalar electric potential in this scenario.

$$\emptyset=\left(\frac{x}{(x^2+(y+a)^2)}\right)\frac{\alpha'}{2\pi} \tag{5}$$

Here, '$\alpha'$' represents the electric field strength at the source. The components of the electric field 'E' are delineated as follows.

$$E_x=-\frac{\partial\emptyset}{\partial x}=\frac{\alpha'}{2\pi}\left(\frac{x^2-(y+a)^2}{x^2+(y+a)^2}\right) \tag{6}$$

$$E_y=-\frac{\partial\emptyset}{\partial y}=\frac{\alpha'}{2\pi}\left(\frac{2x(y+a)}{x^2+(y+a)^2}\right) \tag{7}$$

$$E=\left[\left(\frac{\partial\emptyset}{\partial x}\right)^2+\left(\frac{\partial\emptyset}{\partial y}\right)^2\right]^{\frac{1}{2}} \tag{8}$$

The relationship between polarization 'P' and temperature 'T' is approximated by a linear equation

$$P = \varepsilon_0(\varepsilon_r - 1) \tag{9}$$

Here, $\varepsilon_0$ and $\varepsilon_r$ represent the absolute and relative dielectric permittivity, respectively.

### 1.1 Solution Procedure

Andersson [10] considered the following non-dimensional variables

$$(\xi,\eta) = \left(\frac{c}{\nu}\right)^{\frac{1}{2}}(x,y), \qquad (U,V) = \frac{(u,v)}{\sqrt{c\nu}} \tag{10}$$

$$\theta(\xi,\eta) = \frac{T_c - T}{T_c - T_w} = \theta_1(\eta) + \xi^2\theta_2(\eta)\ in\ PST\ case \tag{11}$$

Where, $T_c - T_w = A\left(\frac{x}{L}\right)\ in\ PST\ case$ (12)

Utilizing equations (9) to (12), the boundary layer equations (1-3) take on the following structure:

$$\frac{\partial U}{\partial \xi} + \frac{\partial V}{\partial \eta} = 0 \tag{13}$$

$$U\frac{\partial U}{\partial \xi} + V\frac{\partial U}{\partial \eta} + \lambda_1 c\left[U^2\frac{\partial^2 U}{\partial \xi^2} + v^2\frac{\partial^2 U}{\partial \eta^2} + 2UV\frac{\partial^2 U}{\partial \xi\,\partial \eta}\right] = \frac{\partial^2 U}{\partial \eta^2} - \frac{2\beta\xi}{(\eta+\alpha)^4}(\theta_1 + \xi^2\theta_2) + G_r\xi sin\theta(\theta_1 + \xi^2\theta_2) \tag{14}$$

$$\Pr[2U\xi\theta_2 + V(\theta_1' + \xi^2\theta_2')] = \theta_1'' + \xi^2\theta_2'' - \lambda\left(\left(\frac{\partial U}{\partial \eta}\right)^2 + 2\left(\left(\frac{\partial V}{\partial \eta}\right)^2\right)\right) \tag{15}$$

The boundary condition described in (4) is now specified as follows:

$U(\xi,0)=\xi$, $V(\xi,0)=0$ and $\theta_1(\xi,0)=1$, $\theta_2(\xi,0)=0$ in PST (16)

Introducing the stream function $(\xi,\eta)=\xi f(\eta)$ yields the following result:

$$U = \frac{\partial \Psi}{\partial \eta} = \xi f'(\eta), \qquad V = \frac{\partial \Psi}{\partial \xi} = -f(\eta) \tag{17}$$

The prime symbol signifies differentiation with respect to η.

Applying equations (9), (11), and (17) within equations (14) and (15) results in the following boundary value problem.

$$f'''(1-\gamma_1) - f'^2 + ff'' + 2\gamma_1 ff'f'' - \frac{2\beta\theta_1(\eta)}{(\eta+\alpha)^4} + Gr\theta_1 sin\theta = 0 \tag{18}$$

$$\theta_1'' - 2\lambda f'^2 + Prf\theta_1' = 0 \tag{19}$$

$$\theta_2'' - \Pr(2f'\theta_2 - f\theta_2') - \lambda f''^2 = 0 \tag{20}$$

At the sheet, the dimensionless form of the shear stress, which represents the local skin friction coefficient denoted by, is expressed as:

$$C_f = \frac{-2\tau_{xy}}{\rho(cx)^2} = -2f''(0)Re_x^{\frac{-1}{2}}$$

When setting the surface temperature, it becomes feasible to compute the local heat flux, given by:

$$Nu_x = -Re_x^{\frac{1}{2}}[\theta_1'(0) + \xi^2\theta_2'(0)]$$

equations (18), (19), and (20) lead to two-point boundary value problems, tackled through both the shooting technique and the Runge-Kutta Fehlberg (RKF45) method. Adjusting the trial values of $f'(0)$, $\theta_1'(0)$, $\theta_2'(0)$ to satisfy the outer boundary conditions involves using the Newton-Raphson approach.

## 2.0 Result and Discussion

The study explores the influence of altering parameters β, Pr and $\gamma_1$, Gr, and θ, on the flow and heat transfer characteristics of viscoelastic dielectric liquid over an inclined stretching sheet. These effects are examined under prescribed temperature boundary conditions, α=1 and λ=0.01 illustrated through graphical representations.

Raising β intensifies the electric field produced by an electric dipole, amplifying friction within the fluid. This increased friction impedes the flow, leading to decreased velocity shown in Figure 2 of the velocity profile, resulting in a flatter profile. Similarly, as illustrated in Figure 2 of the temperature profile, higher values of the

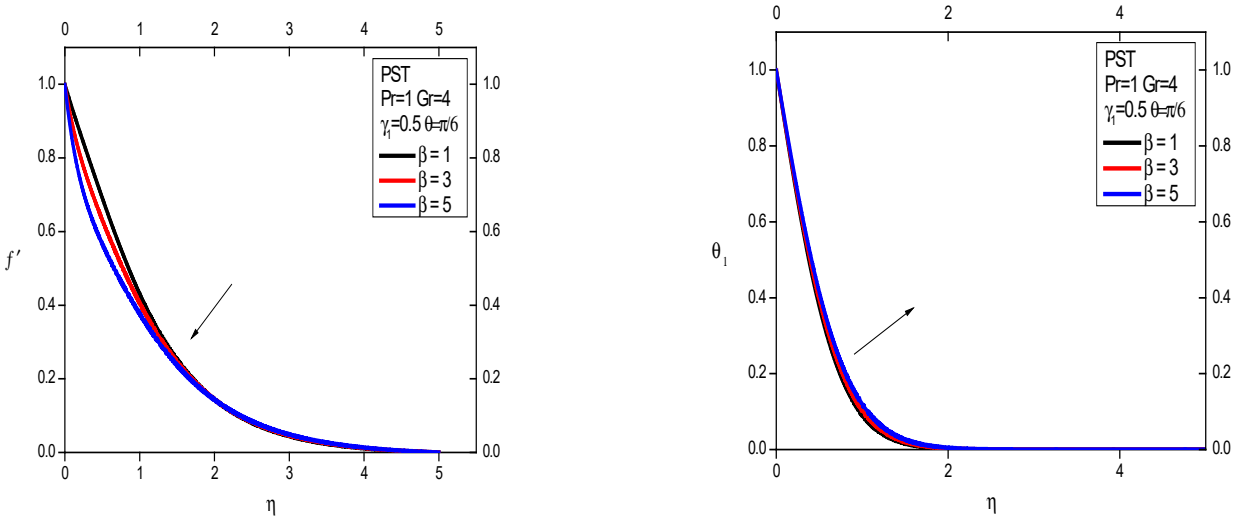


**Figure 2.** Showing profile f'(η) and Temperature profile $\theta_1$ for various values of β.

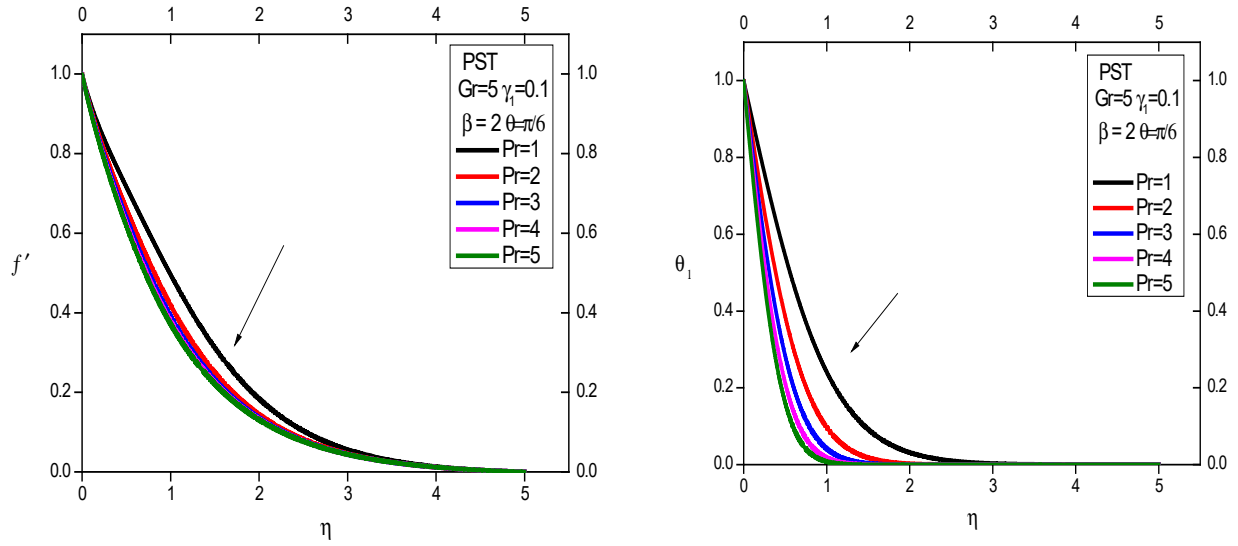


**Figure 3.** Velocity profile f'(η) and Temperature profile $\theta_1$ for various values of Pr.

dielectric interaction parameter β impact the temperature distribution. Elevated β values correlate with a thicker thermal boundary layer within the Prescribed Surface Temperature boundary (PST).

Positive variations in the Prandtl number (Pr) exhibit a corresponding decrease in velocity due to the increased viscosity of the fluid. As depicted in Figure 3, the impact of Pr values on velocity boundary layers showcases this trend. Such findings hold substantial significance across numerous dielectric applications, spanning crystal formation, metal processing, nuclear reactors, metallurgy, fiber spinning, casting, and space technologies.

Moreover, Figure 3 vividly illustrates that fluids with lower Prandtl numbers exhibit more efficient reduction in heat transmission.

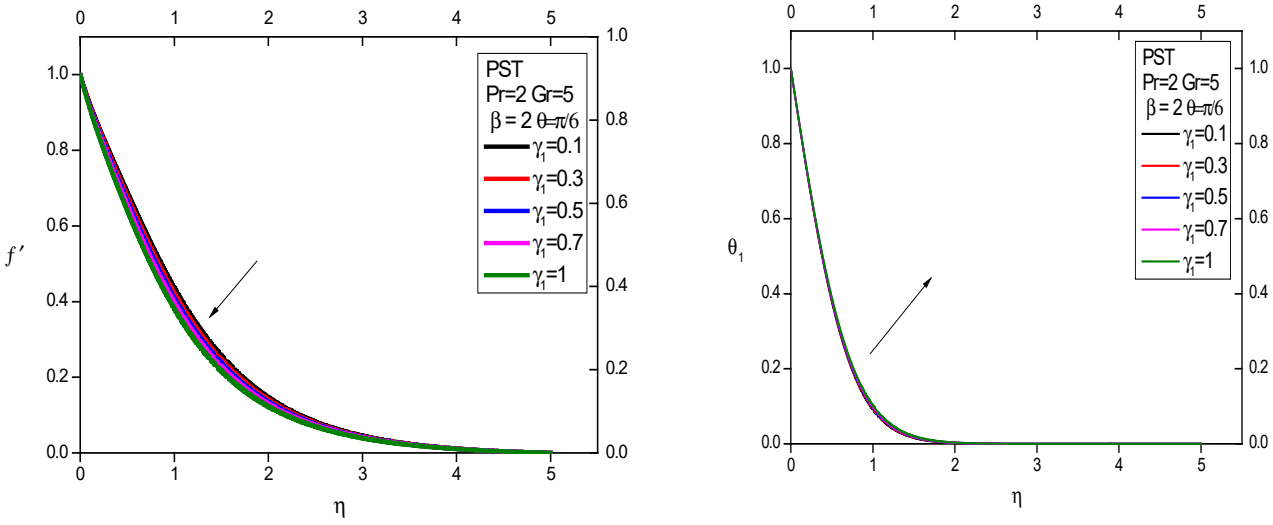


**Figure 4.** Velocity profile f'(η) and Temperature profile $\theta_1$ for various values of $\gamma_1$

In Figure 4, the impact of Viscoelastic parameter ($\gamma_1$) on velocities profile f'(η) under prescribed surface temperature profile ($\theta_1$) (PST) conditions is evident. The significance of convection in influencing axial velocity is emphasized by varying ($\gamma_1$). The depicted graphs illustrate that as ($\gamma_1$) increases, the thickness of the momentum boundary layer expands, enabling freer fluid flow.

Moreover, the flow exhibits boundary layer characteristics. Figure 4 portrays the influence of on heat transmission, revealing that an increase in Viscoelastic parameter heightens the temperature profile $\theta_1$. This arises from the thickening of the thermal boundary layer due to viscoelastic normal stress.

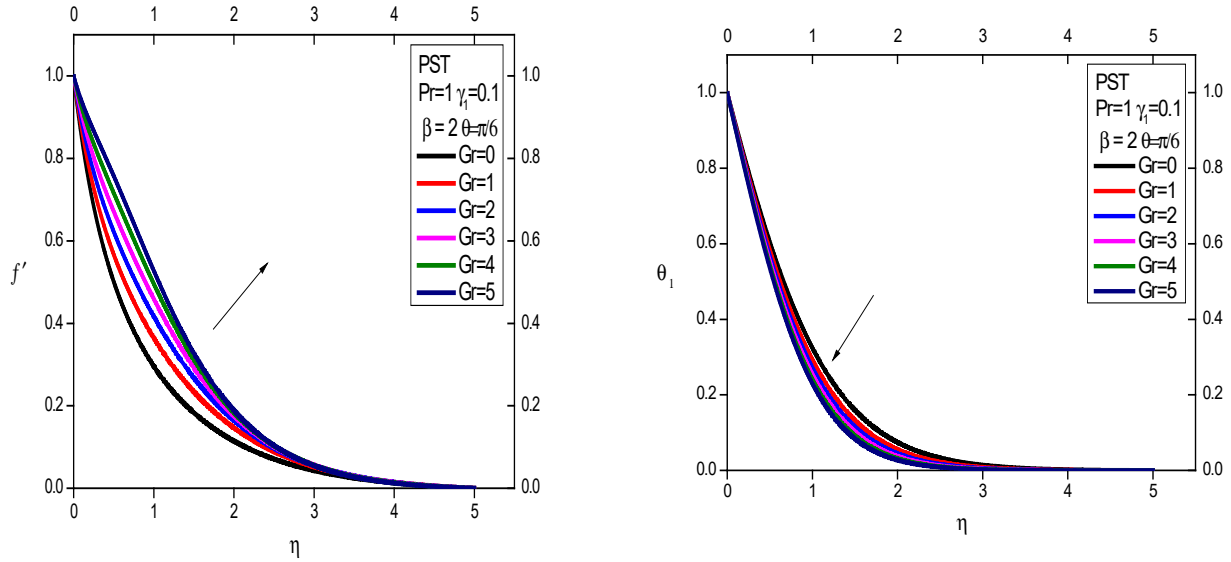


**Figure 5.** Temperature profile f'(η) and Temperature profile $\theta_1$ for various values of Gr.

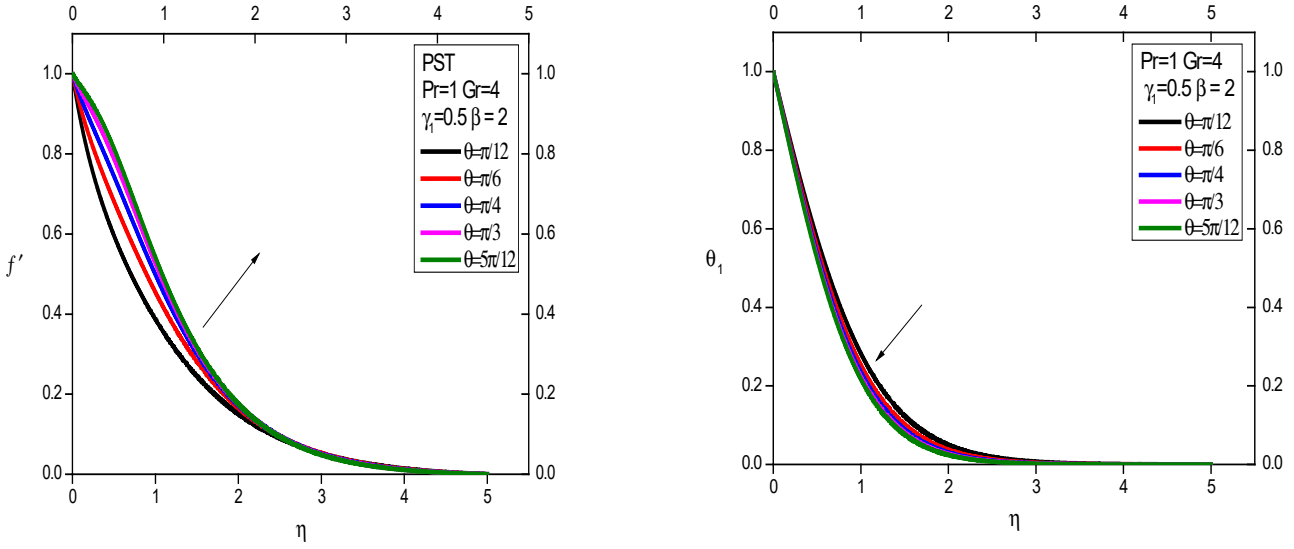


**Figure 6.** Temperature profile f'(η) and Temperature profile $\theta_1$ for for various values of θ.

The Grashof number (Gr) is approximated by the product of the buoyancy force and viscous shear force acting on a given fluid. When Gr is increased, momentum boundary layer thickness increases, resulting in 0% pressure gradient across the flow surface. This can be observed in Figure 5 of velocity profile f'(η). The buoyancy force has evolved as a consequence of the cooled yielding sloping layer acting like a positive pressure gradient to

**Table 1.** For different values of non-dimensional parameters local Nusselt number and Skin friction.

| Pr | β | Gr | $\gamma_1$ | Nusselt number | Skin friction |
|---|---|---|---|---|---|
| 1 | | | | 0.6897229 | 1.53914 |
| 3 | | | | 1.214584 | 1.932682 |
| 5 | | | | 1.595581 | 2.071728 |
| | 0 | | | 0.7179273 | 0.359406 |
| | 3 | | | 0.6746989 | 2.391956 |
| | 5 | | | 0.6424735 | 3.793102 |
| | | 0 | | 0.5279590 | 3.603328 |
| | | 1 | | 0.5934216 | 2.985272 |
| | | 3 | | 0.6644199 | 1.986708 |
| | | | 0.1 | 0.6897229 | 1.53914 |
| | | | 0.2 | 0.6837137 | 1.58119 |
| | | | 0.3 | 0.6779828 | 1.62306 |

**Table 2.** Validation of current findings using previously published works in a restricted number of cases when

| Pr | Reference[33] | Reference[34] | Current findings |
|---|---|---|---|
| 1 | 0.58199 | 0.5820 | 0.5819 |
| 3 | 1.16523 | 1.1652 | 1.1652 |
| 10 | 7.76536 | 7.7657 | 7.7653 |

accelerate the fluid in the boundary layer region. This also results in decreasing the temperature profile $\theta_1$ which can be observed in Figure 5.

Despite the various factors that influence viscosity, a higher inclination results in greater momentum boundary layer thickness, when gravity is increased the liquid flows freely. The thermal boundary layer thickness is decreased by the inclination. Figure 6 shows this in more detail provides a view on $f'(\eta)$ and $\theta_1(\eta)$.

## 3.0 Conclusion

This paper investigates the behavior of a viscoelastic dielectric liquid over an inclined stretched sheet, yielding several key findings:

- The Prandtl number (Pr) influences boundary layer thickness, dictating the mechanism of heat transfer. A higher Pr leads to a wider velocity boundary layer compared to the temperature boundary layer, resulting in reduced heat transfer—an aspect critical for system performance.
- Both Grashof and Prandtl numbers contribute to enhancing flow and heat transfer, thereby reducing thermal heat.
- Optimal cooling requires maintaining these parameters at their minimum values to ensure efficient heat dissipation.
- As gravity gets more powerful, the stretching sheet's angle of inclination to the horizontal, as well as the thickness of the momentum boundary layer, all increase. The quantity of heat that may enter or leave is constrained by the inclination.
- When the angle $\theta$ equals zero, the inclined stretching sheet scenario simplifies into the horizontal stretching sheet problem. Similarly, setting $\theta$ to $\pi/2$ transforms the inclined stretching sheet problem into the vertical stretching sheet case.
- The result shows that for achieving desired temperature inclination of stretching sheet can be used effectively.
- The combination of dielectric liquids and inclined stretching sheets finds applications in various processes such as separation, material fabrication, and optimization of fluid behaviour, leading to improved efficiency, control, and performance in mining, materials, and fuel-related operations.

## 4.0 Acknowledgement

We thank S J C Institute of Technology, Chickballapur, BMSIT&M, Bangalore as well as M.S. Ramaiah Institute of Technology, Bangalore for their support and encouragement.

## 5.0 References

1. Fisher EG. Extrusion of plastics. 3rd ed. London: Newnes-Buttterworld; 1976.
2. Sakiadis BC. Boundary-layer behaviour on continuous solid surfaces I: The boundary layer on equations for two-dimensional and axisymmetric flow. AIChE J. 1961; 7(1):26-28.
3. Sakiadis BC. Boundary-layer behavior on continuous solid surfaces II: The boundary layer on a continuous flat surface. AIChE J. 1961; 7(1):221-225.
4. Sakiadis BC. Boundary-layer behavior on continuous solid surfaces III: The boundary layer on a continuous cylindrical surface. AIChE J. 1961; 7(1):467-472.
5. Tsou FK, Sparrow EM, Goldstein RJ. Flow and heat transfer in the boundary layer on continuous moving surfaces. Int J Heat Mass Transfer. 1967; 10(2):219-235.

6. Crane LJ. Flow past a stretching plate. J Appl Math Phys (ZAMP). 1970; 21:645-647.
7. Siddappa B, Subhash AM. Non-Newtonian flow past a stretching plate. Z Angew Math Phys. 1985; 36:890.
8. Rajagopal KR, Na TY, Gupta AS. Flow of a viscoelastic fluid over a stretching sheet. Rheol Acta. 1984; 23:213.
9. Dandapat BS, Gupta AS. Flow and heat transfer in a viscoelastic fluid over a stretching sheet. Int J Non-Linear Mech. 1989; 24(3):215.
10. Andersson HI. Slip flow past a stretching surface. Acta Mech. 2002; 158(1-2):121-125.
11. Rollins D, Vajravelu K. Heat transfer in a second-order fluid over a continuous stretching surface. Acta Mech. 1991; 89:167.
12. Kelly D, Vajravelu K, Andrews L. Analysis of heat mass transfer of a viscoelastic, electrically conducting fluid past a continuous stretching sheet. Nonlinear Anal. 1999; 36:767.
13. Bhatnagar RK, Rajagopal KR, Gupta AS. Flow of an Oldroyd B model due to a stretching sheet in the presence of a free stream velocity. Int J Non-Linear Mech. 1995; 30:391.
14. Othman MIA. Electrohydrodynamic stability in a horizontal viscoelastic fluid layer in the presence of a vertical temperature gradient. Int J Eng Sci. 2001; 39:1217–1232.
15. Siddheshwar PG, Annamma Abraham. Rayleigh-Benard Convection in a Dielectric Liquid: Imposed Time-Periodic Boundary Temperatures. Chamchuri J Math. 2009; 1(2):105-121. [Online].
16. Siddheshwar PG, Abraham A. Rayleigh-Benard Convection in a Dielectric liquid: Time-periodic body force. PAMM. 2008; 7(1):2100083-2100084.
17. Siddheshwar PG, Revathi BR. Effect of Gravity Modulation on Weakly Non-Linear Stability of Stationary Convection in a Dielectric Liquid. World Acad Sci Eng Technol. 2013; 7:2013-01-23.
18. Annamma Abraham. Rayleigh-Benard-Marangoni Instability In A Micro-Polar Dielectric Liquid Using The Galerkin Technique. Math Sci Int Res J. 2013; 2(2):254-258.
19. Titus LS, Abraham Annamma. Flow of Ferrofluid Over an Inclined Stretching Sheet in the Presence of a Magnetic Dipole. 2019. DOI: 10.1007/978-981-32-9531-5_4.
20. Zeb H, Wahab HA, Khan U, Juhani ASA, Andualem M, Khan I. The Velocity Slip Boundary Condition Effects on Non-Newtonian Ferrofluid over a Stretching Sheet. Math Probl Eng. 2022; 2022. DOI: 10.1155/2022/1243333.
21. Alhadhrami A, Prasanna BM, Rajendra KC, Sarada K, Alzahrani H. Heat and Mass Transfer Analysis in Chemically Reacting Flow of Non-Newtonian Liquid with Local Thermal Non-Equilibrium Conditions: A Comparative Study. Energies. 2021; 14:5019. DOI: 10.3390/en14165019.
22. Saleh B, Madhukesh JK, Kumar RS Varun, Afzal A, Abdelrhman Y, Aly A, Punith Gowda RJ. Aspects of magnetic dipole and heat source/sink on the Maxwell hybrid nanofluid flow over a stretching sheet. Proc Inst Mech Eng E J Process Mech Eng. 2022. DOI: 10.1177/09544089211056243.
23. Punith Gowda RJ, Sarris I, Kumar R, Prasannakumara BC. A Three-Dimensional Non-Newtonian Magnetic Fluid Flow Induced Due to Stretching of the Flat Surface With Chemical Reaction. J Heat Transfer. 2022. DOI: 10.1115/1.4055373.
24. Awucha UU, Amos E, Nwaigwe C. Chemical Reaction and Thermal Radiation Effects on Magnetohydrodynamic Nanofluid Flow Past an Exponentially Stretching Sheet. Theor Math Appl. 2022. DOI: 10.47260/tma/1221.
25. Suraiah Palaiah S, Basha H, Reddy GJ, Sheremet MA. Magnetized Dissipative Soret Effect on Chemically Reactive Maxwell Fluid over a Stretching Sheet with Joule Heating. Coatings. 2021; 11:528. DOI: 10.3390/coatings11050528.
26. Conductivity VT, Effects D, Jawad M. Analytical Study of MHD Mixed Convection Flow for Maxwell Nanofluid with Analytical study of MHD mixed convection flow for Maxwell nanofluid with variable thermal conductivity and Soret and Dufour effects. 2021. DOI: 10.1063/5.0029105.
27. Punith Gowda RJ, Naveen Kumar R, Prasannakumara BC, Nagaraja B, Gireesha BJ. Exploring magnetic dipole contribution on ferromagnetic nanofluid flow over a stretching sheet: An application of Stefan blowing. J Mol Liquids. 2021; 335:116215. DOI: 10.1016/j.molliq.2021.116215.
28. Kumar R, Jyothi A, Alhumade H, Punith Gowda RJ, Alam MM, Ahmad I, Gorji MR, Prasannakumara BC. Impact of magnetic dipole on thermophoretic particle deposition in the flow of Maxwell fluid over a stretching sheet. J Mol Liquids. 2021; 334:116494. DOI: 10.1016/j.molliq.2021.116494.
29. Madhukesh JK, Alam MM, Varun Kumar RS, Arasaiah A, Ahmad I, Gorji MR, Prasannakumara BC. Exploring magnetic dipole impact on Maxwell hybrid nanofluid flow

over a stretching sheet. Proc Inst Mech Eng E J Process Mech Eng. 2022. DOI: 10.1177/09544089211073267.
30. Shagaiya Y, Abdul Z, Ismail Z, Salah F. Thermal radiation on unsteady electrical MHD flow of nanofluid over stretching sheet with chemical reaction. J King Saud Univ Sci. 2019; 31(4):804–812. DOI: 10.1016/j.jksus.2017.10.002.
31. Prasannakumara BC. Partial Differential Equations in Applied Mathematics Numerical simulation of heat transport in Maxwell nanofluid flow over a stretching sheet considering magnetic dipole effect. Partial Differential Equations in Applied Mathematics. 2021; 4:100064. DOI: 10.1016/j.padiff.2021.100064.
32. Veena N, Dinesh PA, Annamma Abraham, Jojy Joseph Idicula. Viscoelastic dielectric liquid flow over a horizontal stretching sheet. [Online] 2023. DOI: 10.1007/s10973-023-12480-y.
33. Chen CH. Laminar mixed convection adjacent to vertical, continuously stretching sheets. Heat Mass Transfer. 1998; 33:471–476.
34. Grubka LJ, Bobba KM. Heat Transfer Characteristics of a Continuous, Stretching Surface with Variable Temperature. Int J Heat Mass Transfer. 1985; 107(1):248-250.

## List of Symbols

| a | Distance | P | Dielectric Polarizaton |
|---|---|---|---|
| $c_p$ | Specific heat constant | $\varepsilon_0$ | Electric permeability of free space |
| k | Thermal conductivity | $T_c$ | Curie temperature |
| (u,v) | Velocity components | ρ | Fluid Density |
| (x,y) | Carsesian component | Ø | Electric potential |
| $Pr = \frac{\mu c_p}{k}$ | Prandtl number | Ψ | Stream function |
| $\lambda = \frac{c\mu}{\rho k(T_c - T_w)}$ | Viscous dissipation | $\lambda_1$ | Relaxation time |
| $\beta = \frac{\alpha'\rho}{2\pi\mu^2}\epsilon_0 e(T_c - T)\Big)$ | Dielectric interaction Parameter | $\gamma_1$ | Viscoelastic parameter |
| μ | Viscosity | α | Dimensionless Distance |
| T | Fluid temperature | | |
| E | Electric field | g | Acceleration due to gravity |